

Phase Transitions in Self-Dual Ising Models with Multispin Interactions and a Field

J. R. Heringa, H. W. J. Blöte, and A. Hoogland

Laboratorium voor Technische Natuurkunde, Lorentzweg 1, 2628 CJ Delft, The Netherlands

(Received 28 April 1989)

We investigate some two- and three-dimensional Ising models with multispin interactions and a field, by means of Monte Carlo simulations. The phase diagram of these models contains a self-dual line, along which we have searched for the presence of a phase transition. In both two and three dimensions we give examples exhibiting a first-order transition along a part of the self-dual line. These first-order lines end in critical points, which are classified as Ising-type in terms of universality. A lattice-gas interpretation of these models clearly shows their similarity with gas-liquid systems.

PACS numbers: 05.50.+q, 64.60.Cn, 64.70.Fx, 75.40.Mg

We consider a general class of d -dimensional, simple hypercubic Ising models with multispin couplings and a field described by the reduced Hamiltonian

$$\frac{\mathcal{H}}{kT} = -K \sum_{\mathbf{r}} \prod_{i=0}^{n-1} S_{\mathbf{r}+\mathbf{a}_i} - H \sum_{\mathbf{r}} S_{\mathbf{r}}. \tag{1}$$

The spin position vectors \mathbf{r} have d arbitrary integer components. The n vectors \mathbf{a}_i specify the multispin interactions. Their components are integers, too. The spins $S_{\mathbf{r}}$ have the value $+1$ or -1 . The factor $1/kT$ has been absorbed in the multispin coupling K and the field H . We restrict ourselves to positive values of H and K .

In order to obtain a clue to the phase diagram in the K - H plane, we have applied mean-field theory to (1). For $n > 2$, this theory predicts the existence of a first-order line ending in a critical point (see Fig. 1, broken line, for the case $n=4$).

More information about the possible location of a phase transition follows from the fact that the models described by (1) are self-dual.¹ In the thermodynamic limit the reduced free energy per site,

$$f(K, H) = \lim_{N \rightarrow \infty} N^{-1} \ln \sum_{\{S\}} \exp(-\mathcal{H}/kT), \tag{2}$$

satisfies the duality relation

$$f(K, H) = \frac{1}{2} \ln(\sinh 2K \sinh 2H) + f(\tilde{K}, \tilde{H}), \tag{3}$$

where the dual field \tilde{H} and the dual coupling \tilde{K} are defined by

$$\sinh 2K \sinh 2\tilde{H} = \sinh 2H \sinh 2\tilde{K} = 1. \tag{4}$$

The points on the self-dual line, given by

$$\sinh 2K \sinh 2H = 1, \tag{5}$$

are invariant under the duality transformation. Thus, if the model exhibits a single phase transition, it is located on the self-dual line (see Fig. 1). Furthermore, it is possible to show² that there is no phase transition for sufficiently small K . A very simple model in the class given by (1) is the Ising chain in a magnetic field, for which it is easy to check the validity of (3). A phase

transition, however, is absent for finite K .

In this Letter, we investigate six less trivial models in two and three dimensions by means of the Monte Carlo method. Since rather long simulations are necessary as a consequence of slow relaxation, we have made use of the DISP (Delft Ising System Processor), a special-purpose computer for the simulation of Ising models.^{3,4} It was built in 1982 by one of us (A.H.). This device runs at a speed slightly over 10^6 spin update attempts per second and is able to simulate a wide class of Hamiltonians. Lattice sizes are restricted to powers of 2. During the simulation the processor keeps track of the lattice sums conjugate to K and H without loss of time. Since long simulations require good pseudorandom numbers, the

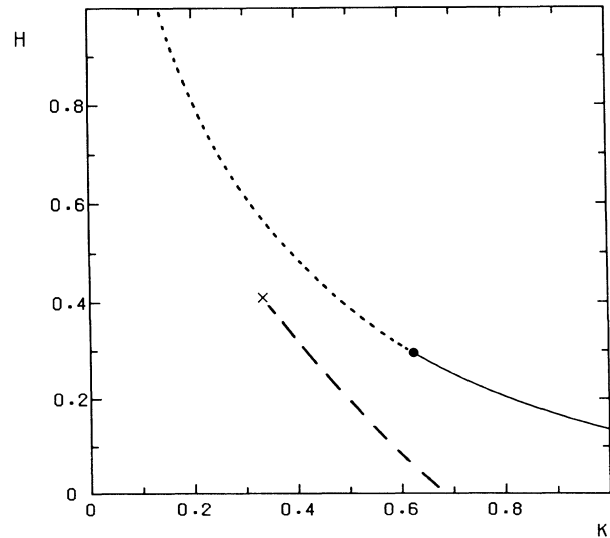


FIG. 1. Phase diagram of model 2. The broken line shows the mean-field prediction: a first-order line ending in a critical point (\times). The self-dual line is shown by the full and the dotted lines. The full part shows the first-order line as found by the Monte Carlo simulations. The critical point (\bullet) separates the first-order range from the range where a transition is absent (dotted line).

random-number generator has been the subject of special care.⁵

The models under investigation are characterized by the lattice dimensionality d and the multispin coupling. For easy reference, they are labeled 1 to 6.

(1) $d=3$, $n=5$, $\mathbf{a}_0=(0,0,0)$, $\mathbf{a}_1=(1,0,0)$, $\mathbf{a}_2=(0,1,0)$, $\mathbf{a}_3=(1,1,0)$, and $\mathbf{a}_4=(0,0,1)$. This model can be trivially reformulated on the body-centered-cubic lattice; the five-spin couplings then occur in the elementary pyramids pointing upward.

(2) $d=3$, $n=4$, $\mathbf{a}_0=(0,0,0)$, $\mathbf{a}_1=(1,0,0)$, $\mathbf{a}_2=(0,1,0)$, and $\mathbf{a}_3=(0,0,1)$. This model can be equivalently formulated on the face-centered-cubic lattice. The four-spin interactions then occur in all elementary tetrahedra with a given orientation (there are two possible orientations).

(3) $d=2$, $n=5$, $\mathbf{a}_0=(0,0)$, $\mathbf{a}_1=(1,0)$, $\mathbf{a}_2=(0,1)$, $\mathbf{a}_3=(-1,0)$, and $\mathbf{a}_4=(0,-1)$. On the square lattice, the multispin interactions couple each spin to its four nearest neighbors.

(4) $d=2$, $n=4$, $\mathbf{a}_0=(0,0)$, $\mathbf{a}_1=(1,0)$, $\mathbf{a}_2=(0,1)$, and $\mathbf{a}_3=(-1,-1)$. When we place this model on the triangular lattice, the four-spin interactions take the "Y" shape.

(5) $d=2$, $n=4$, $\mathbf{a}_0=(0,0)$, $\mathbf{a}_1=(1,0)$, $\mathbf{a}_2=(0,1)$, and $\mathbf{a}_3=(1,1)$. These four-spin interactions couple the spins of the elementary faces of the square lattice.

(6) $d=2$, $n=3$, $\mathbf{a}_0=(0,0)$, $\mathbf{a}_1=(1,0)$, $\mathbf{a}_2=(0,1)$. On the triangular lattice, the three-spin interactions couple the spins of the elementary up triangles.

As a first step, we have determined the energy of these models as a function of K for several values of H/K in the neighborhood of the self-dual line. We have used system sizes up to 32^3 ($d=3$) and 64^2 ($d=2$). For models 5 and 6 the energy has been found to depend continuously on K , for $H/K \gtrsim 0.14$. For smaller H/K , the relaxation time becomes very long, inhibiting further conclusions. For models 1-4, however, clear discontinuities in the energy are apparent on the self-dual line for sufficiently small H/K . For larger values of H/K , the energy behaves continuously and is nearly independent of the system sizes. As an example we show some of the results for model 1 in Figs. 2(a) and 2(b). The behavior of models 2-4 is found to be qualitatively similar.

In order to locate the expected critical point at the end of the first-order line, we have determined the magnetization distribution and calculated the quantity

$$Q(L,H) = \langle (m - \bar{m})^2 \rangle / \langle (m - \bar{m})^4 \rangle \quad (6)$$

along the self-dual line for several values of the linear size L of the system. Here m denotes the magnetization per spin ($-1 \leq m \leq 1$) and \bar{m} is the average of m . Along the first-order line we expect $Q(L,H) \rightarrow 1$ for $L \rightarrow \infty$, while $Q(L,H) \rightarrow \frac{1}{3}$ where a phase transition is absent. Scaling arguments^{6,7} predict that at the critical point, which separates both ranges of the self-dual line, $Q(L,H)$ converges to a universal constant Q_c (between

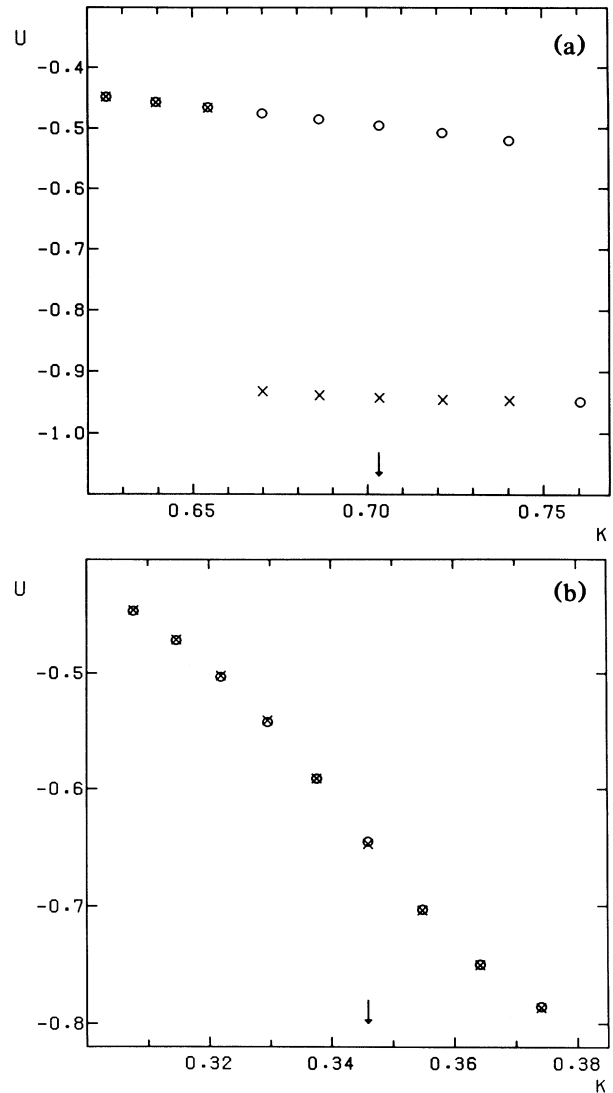


FIG. 2. Energy of model 1 vs the multispin coupling K (a) for $H/K=0.3554$ and (b) for $H/K=1.5893$. The system size is $L=16$; (a) and (b) have been found to depend only weakly on (not too small) L . The symbols indicate the way in which K is varied: \circ , K increasing; \times , K decreasing. The arrows show the value of K for which (K,H) is self-dual. The statistical errors are less than the size of the symbols. (a) indicates a first-order transition, (b) the absence of a transition.

$\frac{1}{3}$ and 1). Thus, the intersections of the $Q(L,H)$ vs H curves for subsequent values of L may serve to estimate the critical field H_c . Figure 3 shows the results for $Q(L,H)$ from the simulation of model 2, with $L=4, 8, 16$, and 32 . A typical number of sweeps used for the lowest value of H is 10^7 , while lattice sums have been accumulated at intervals of twenty sweeps. The data shown in Fig. 3 indicate the existence of a critical point at $H_c=0.295(1)$. Similar analyses have been performed on models 1, 3, and 4; the results in terms of H_c and Q_c

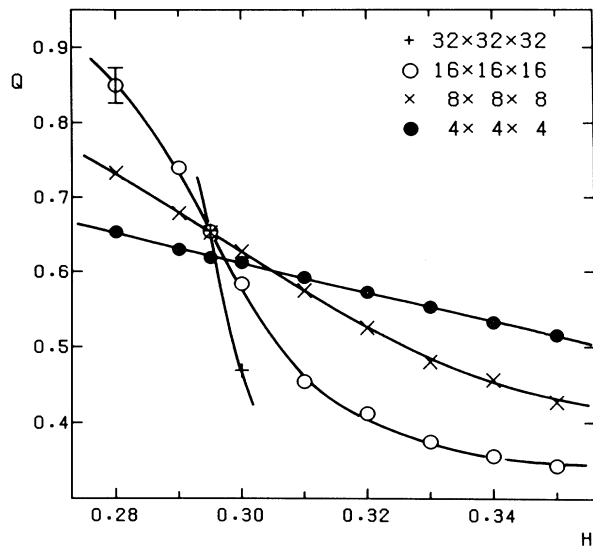


FIG. 3. The quantity Q [defined in Eq. (6)] of model 2 vs H along the self-dual line for a number of system sizes L . The curves serve only as guides to the eye. Where no error is shown, the statistical errors are less than or equal to the size of the symbols. The intersection points serve to estimate the critical point and the critical ratio of Q_c .

are summarized in Table I.

Another method to determine the location of a critical point uses the finite-size dependence of the susceptibility $\chi(L, H)$. Neglecting corrections to scaling, we have, at criticality,

$$\chi(L, H_c) \sim L^{2Y_H - d}, \quad (7)$$

where Y_H is the magnetic exponent. Using subsequent system sizes L and $2L$,

$$\frac{1}{2} \left(\frac{\log[\chi(2L, H_c)/\chi(L, H_c)]}{\log 2} + d \right) = Y_H. \quad (8)$$

In Fig. 4 we use model 3 as an example, and plot the left-hand side of (8) versus H along the self-dual line for subsequent values of L . The values of H in the intersection points serve as estimates of H_c . They agree satisfactorily with the aforementioned results from the magnetization distribution. The results for H_c presented in Table I are derived from the combination of both analyses.

Similar analyses for models 1, 2, and 4 lead to similar conclusions. The observed finite-size dependence of the H_c estimates is less pronounced for model 2. The results in terms of Y_H are included in Table I.

The results for Q_c may be compared to the universal values $Q_c = 0.856$ and 0.62 for the $d=2$ Ising model⁸⁻¹⁰ and the $d=3$ Ising model,¹¹ respectively. Furthermore, the magnetic exponent $Y_H = \frac{15}{8}$ for the $d=2$ Ising model¹² and $Y_H = 2.484(6)$ for the $d=3$ Ising model.¹³ This comparison shows that the critical behavior of the

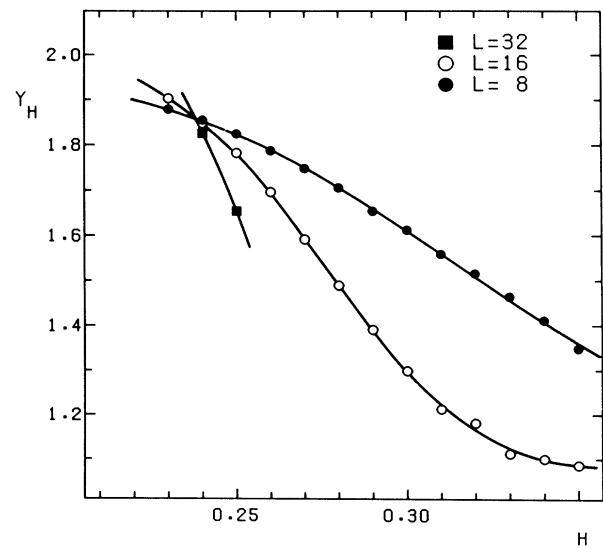


FIG. 4. Left-hand side of Eq. (8) for model 3 vs the field H along the self-dual line for three systems sizes L . The curves serve only as guides to the eye. The statistical errors are less than or equal to the size of the symbols. The intersections yield estimates of the critical point as well as the magnetic exponent Y_H .

present models agrees with that of the appropriate Ising universality class. In order to appreciate this classification, note that the usual Ising symmetry, which connects positively and negatively magnetized states on the phase transition line, is absent in the present models described by (1). The observed first-order lines separate two states with different, but positive, magnetizations. These states may be interpreted as "dilute" and "dense," according to the density of + spins. In this lattice-gas interpretation, our models 1-4 are similar to gas-liquid systems, which also have a first-order line, which separates a dilute from a dense phase, and which ends in a presumably Ising-type critical point.¹⁴ The equiva-

TABLE I. Critical-point data for models 1-6. For models 5 and 6 our results are consistent with the absence of phase transitions. Shown are the results for the reduced critical field H_c , the dimensionless ratio Q_c of moments of the magnetization distribution, and the magnetic exponent Y_H . The methods used for their determination are described in the text. Also shown is the total number of elementary Monte Carlo steps performed for each model.

Model	H_c	Q_c	Y_H	No. Monte Carlo steps
1	0.378(3)	0.64(2)	2.50(5)	2.9×10^{11}
2	0.295(1)	0.65(2)	2.52(5)	8.3×10^{11}
3	0.195(5)	0.83(2)	1.90(5)	3.9×10^{11}
4	0.239(4)	0.84(2)	1.85(5)	6.4×10^{11}
5	< 0.14			6.6×10^{11}
6	< 0.14			8.2×10^{11}

lence with a lattice gas is most easily demonstrated for the case that n is even. We transform the Ising variables into lattice-gas variables $u_r = (1 + S_r)/2$. Then, (1) becomes

$$\frac{\mathcal{H}}{kT} = E_0 + 2(nK - H) \sum_r u_r - 4K \sum_r u_r \sum_{i \neq j} u_{r+a_i - a_j} + \dots, \quad (9)$$

where E_0 is a constant. The second term accounts for the chemical potential of the lattice gas, and the third term for an attractive potential between neighbors as specified. The ellipses stand for higher-order interactions. Our results suggest the existence of a class of models for which these are irrelevant. Such models, defined by (9) [or (1)], belong to the same universality class as the simple lattice gas described by a chemical potential and pair interactions.

It is a pleasure to thank A. Compagner for his essential contributions to the versatility and reliability of the DISP. Thanks are also due to M. Mijnaerends for the construction of hardware for a new lookup table for the DISP, and to J. M. J. van Leeuwen and P. W. Kasteleyn for valuable discussions.

¹C. Gruber, A. Hintermann, and D. Merlini, *Group Analysis of Classical Lattice Systems* (Springer-Verlag, Berlin, 1977), p. 25.

²J. L. Monroe, *J. Stat. Phys.* **33**, 77 (1983).

³A. Hoogland, J. Spaa, B. Selman, and A. Compagner, *J. Comput. Phys.* **51**, 250 (1983).

⁴A. Hoogland, A. Compagner, and H. W. J. Blöte, in *Special Purpose Computers*, edited by B. J. Alder, Computational Techniques Vol. 5 (Academic, New York, 1988).

⁵A. Compagner and A. Hoogland, *J. Comput. Phys.* **71**, 391 (1987).

⁶K. Binder, *Z. Phys. B* **43**, 119 (1981).

⁷A. D. Bruce, *J. Phys. C* **14**, 3667 (1981).

⁸D. P. Landau and K. Binder, *Phys. Rev. B* **31**, 5946 (1985).

⁹A. D. Bruce, *J. Phys. A* **18**, L873 (1985).

¹⁰T. W. Burkhardt and B. Derrida, *Phys. Rev. B* **32**, 7273 (1985).

¹¹M. N. Barber, R. B. Pearson, D. Toussaint, and J. L. Richardson, *Phys. Rev. B* **32**, 1720 (1985).

¹²C. N. Yang, *Phys. Rev.* **85**, 808 (1952).

¹³J. C. Le Guillou and J. Zinn-Justin, *Phys. Rev. B* **21**, 3976 (1980); see also G. A. Baker, B. G. Nickel, and D. J. Meiron, *Phys. Rev. B* **17**, 1365 (1978).

¹⁴See, e.g., S. Ma, *Modern Theory of Critical Phenomena* (Benjamin, Reading, MA, 1976).